Interaction of menthol with mixed-lipid bilayer of stratum corneum: A coarse-grained simulation study

Guang Wan [a,b], Xingxing Dai [b,c], Qianqian Yin [a], Xinyuan Shi [b,c,*], Yanjiang Qiao [b,c,*]

[a] School of Traditional Chinese Medicine, Capital Medical University, Beijing 100069, China
[b] Beijing University of Chinese Medicine, Beijing 100102, China
[c] Key Laboratory of TCM-information Engineer of State Administration of TCM, Beijing 100102, China

ARTICLE INFO

ABSTRACT

Menthol is a widely used penetration enhancer in clinical medicine due to its high efficiency and relative safety. Although there are many studies focused on the penetration-enhancing activity of menthol, the details of molecular mechanism are rarely involved in the discussion. In this study, we present a series of coarse-grained molecular dynamics simulations to investigate the interaction of menthol with a mixed-lipid bilayer model consisting of ceramides, cholesterol and free fatty acids in a 2:2:1 molar ratio. Taking both the concentration of menthol and temperature into consideration, it was found that a rise in temperature and concentration within a specific range (1–20%) could improve the penetration-enhancing property of menthol and the floppiness of the bilayer. However, at high concentrations (30% and more), menthol completely mixed with the lipids and the membrane can no longer maintain a bilayer structure. Our results elucidates some of the molecular basis for menthol's penetration enhancing effects and may provide some assistance for the development and applications of menthol as a penetration enhancer. Furthermore, we establish a method to investigate the penetration enhancement mechanism of traditional Chinese medicine using the mixed-lipid bilayer model of stratum corneum by molecular dynamics simulations.

© 2015 Elsevier Inc. All rights reserved.

1. Introduction

Transdermal drug delivery system is key field in pharmaceutical research. It has several advantages over oral administration, such as bypassed first-pass liver metabolism and gastrointestinal irritation, improved bioavailability, better patient compliance and reduced side effects [1–4]. However, human skin can selectively and effectively inhibits chemical penetration [5]. The most important control element is generally the stratum corneum (SC), whose barrier property hampers the application of transdermal drug delivery [6,7]. Thus, it is important to promote the drug penetration property through SC in the development of transdermal drug delivery procedures.

The most common approach to drug penetration enhancement is through employing permeation enhancers (PEs). Compared with frequently-used chemical PEs (sulfoxides, alcohols, azone etc.), volatile oil of traditional Chinese medicine, especially terpenoids, may offer advantages for being less toxic to the body [8]. Menthol, a monoterpenoid component extracted from traditional Chinese medicine (TCM) *Mentha arvensis* var. *piperasceus*, has traditionally been used for the treatment of febrile diseases, muscle aches, sprains and other similar conditions using alone. In recent years, it has also been widely used as a PE in clinical medications. As previously reported, menthol can efficiently promote the penetration of both hydrophilic and lipophilic drugs, such as quercetin, ondansetron hydrochloride, salicylate, zidovudine, etc. [9–12]. Given the "yaofuheyi" characteristic (means that an agent in a preparation not only have the effect of drug but also can be used as an excipient) and good penetration enhancing efficiency of menthol, it turned out to be a representative volatile oil of TCM used as a PE.

To elucidate the mechanisms of penetration enhancement of menthol, a lot of previous research has been done. Many researchers have inferred from in-vitro transdermal experiments that the penetration enhancement mechanism of menthol is possibly to disrupt and transform the SC lipids from its original state into a less ordered packing form [9,13]. There are also some observations of menthol's effect on skin by various type of microscopy

such as light microscopy, scanning electron microscopy and transmission electron microscopy. [14,15], indicating the rarefaction and shedding of SC caused by menthol. However, the penetration enhancement mechanism of menthol has rarely been discussed from molecular level due to the restrictions of the experimental methods applied and the complexity of the transdermal process. New techniques and methods need to be adopted to gain further insight on this issue.

Molecular dynamics (MD) simulation is an effective and intuitional technique based on Newtonian mechanics. It is becoming increasingly popular in studies on the interactions of molecules within the lipid bilayer systems, providing us with information that cannot be obtained by laboratory experiments [16]. Furthermore, we can explore larger temporal and spatial scales during a simulation by altering molecular resolution, an approach generally known as mesoscopic or coarse-grained (CG) [16,17]. Martini force field, the most widely used CG force field developed by Marrink and his coworkers in 2007, has been widely used in many studies of biomolecules, such as lipids, polymers, proteins, carbohydrates, etc. [18–22]. Several studies have been done to discuss the property and feasibility of different membrane models using Martini CG force field [23–27]. The results show that the loss in chemical specificity of the models can be kept to a minimum under the CG approach and a larger system and longer time-scale can be obtained as well. Therefore, MD simulation using Martini CG force field is an ideal method for investigating the interactions of molecules within bio-membranes and to elucidate the molecular mechanisms of adsorption and penetration.

In this work, a number of MD simulation studies were carried out on a mesoscopic level to investigate the interaction of menthol with a mixed skin-lipid model of SC. Both the concentrations of menthol and temperature effects were taken into consideration, aiming to explain the molecular mechanisms of menthol's penetration enhancing effect and thus provide some assistance for the development and application of menthol as a penetration enhancer.

2. Simulation method

2.1. Force field

All the simulation studies in this work were carried out on a mesoscopic level by CG method to obtain longer time and length scales. The interaction parameters used in the simulation were based on the Martini force field, which was provided by the website of Martini [28]. The Martini model is based on a four-to-one mapping (on average four heavy atoms are represented by a single interaction center), but for ring structures, a two/three-to-one mapping method is used [18]. There are 18 types of normal sites and corresponding S-sites (for ring structures) in Martini force field, which reserves the main information of molecules and attain longer temporal and larger spatial scales in simulation as well.

2.2. Bilayer model of SC

SC is mainly composed of corneocytes and a specialized mixture of lipids, which is often found in a "brick and mortar" form, with the corneocytes (bricks) surrounded by the continuous lipid layers (mortar) [29,30]. The lipids, mainly comprised of ceramides (CER), free fatty acids (FFA) and cholesterol (CHOL), are organized in lamellar layers which are essentially impermeable and thus form the main barrier against penetration [31]. Given the complexity of the composition of the skin lipids and the consensus over their molecular architecture, many researchers have developed skin-lipid 'substitutes' to explore the interaction of molecules within SC using MD simulation, which has a barrier function similar to skin tissue [32]. Both single-component models [33–36] and mixed skin-lipid models with different compositions and contents [37–40] have been investigated. Das et al. demonstrated that the simulated model bilayers comprising of CER2 (ceramide NS, the predominant ceramide in skin lipid with a C24:0 fatty acid tail, short for CER in the following passage), FFA (C24:0) and CHOL at ratio close to 2:2:1 has the most desirable properties of good barrier function and stability against mechanical stress [38,39]. Therefore, it can be used to investigate the interactions and elucidate the molecular mechanisms of the penetration enhancement effect of menthol.

2.3. CG molecule models

This assay mainly involves five molecules, menthol, CER, CHOL, FFA and water. The parameter files of the CG models of CER, CHOL, FFA and water are available in the Martini website (Fig. 1a–d showing the mapping methods respectively), however, menthol has never been parameterized to a CG model.

We developed the CG model of menthol (CG-men) according to the CG recipe published in the Martini website [41], and then validated the new CG-men. The atomistic structure was mapped via Visualizer and Mesocite modules in Materials Studio 5.5 (Accelrys Inc., supported by CHEMCLOUDCOMPUTING) software package [42]. Fig. 1(e) showing the mapping method and some parameters of CG-men. Menthol is a ring-like amphiphilic molecule with a hydrophilic hydroxyl group and some hydrophobic methyl groups. We took a polar bead (SP1) to represent the hydrophilic group and three apolar beads (SC1) to take the place of the hydrophobic parts.

Because the key to developing a new CG model is the 'Coarse-grain target atomistic data', we calculated the bond distributions and radial distribution functions (RDFs) of menthol-octanol in a mixed-system consisting of a certain amount of menthol, water and octanol. Both of them were calculated by all atom (AA) method and CG method to validate our CG-men. RDFs provide a measure of the probability that, given the reference particle α at the origin of an arbitrary reference frame, there will be a particle β with its center located in a spherical shell of infinitesimal thickness at a distance, r, from the reference particle α [42]. Thus, the cumulative number RDF would indicate the total average number of particle β around α within a distance of r [43]. The results show that all the bond distributions (Table 1), the RDFs and cumulative number RDF of menthol–octanol of CG model (Fig. 2) are similar to that in AA representations, which demonstrats our CG-men to be a valid model.

2.4. Initial structures

The bilayer model of SC in this study is composed of CER, CHOL and FFA in a 2:2:1 molar ratio, whose properties have been validated by Das and his coworkers in 2009 [38,39]. The bilayer systems with different menthol concentrations in water are built using the Packmol package [45] and figures depicting lipid molecules are generated with Visual Molecular Dynamics (VMD) [46].

Fig. 3(a) shows a side view of a fragment of the blank bilayer, which packed CER (252 lipids), CHOL (252 lipids), FFA (126 lipids) and water (4882 beads) in a box of $18 \times 18 \times 10$(nm). Next, the
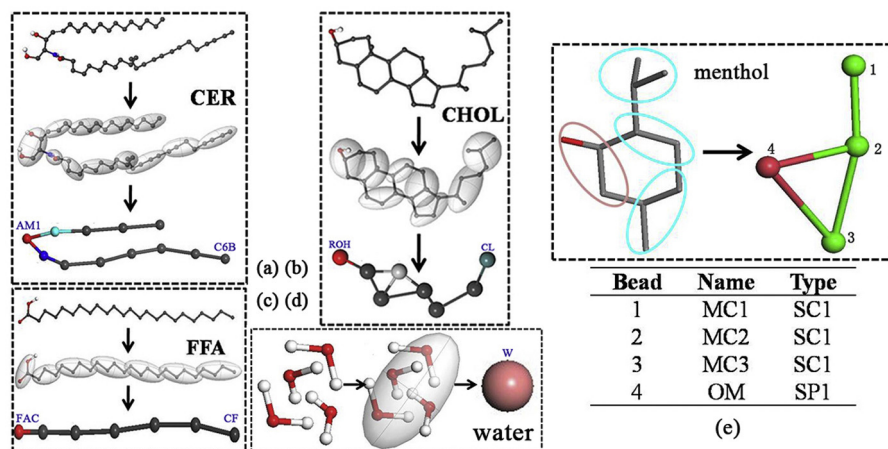
Table 1
Bond distributions of menthol by AA and CG methods.

Bond	AA	CG	RSD[*]%
1–2	0.2483	0.2428	2.2
2–3	0.2892	0.2787	3.6
2–4	0.2490	0.2464	1.0
3–4	0.2903	0.2964	2.1

[*] Relative standard deviation.

Fig. 1. Chemical structures and CG mapping for CER (a), CHOL (b), FFA (c), water (d) and menthol (e). The mapping methods of (a), (b), (c) and (d) are designed according to existing data in the Martini website, and the bead names of some key sites are marked by purple letters. The mapping parameters (bead number, name and force field type) of menthol are shown in (e).
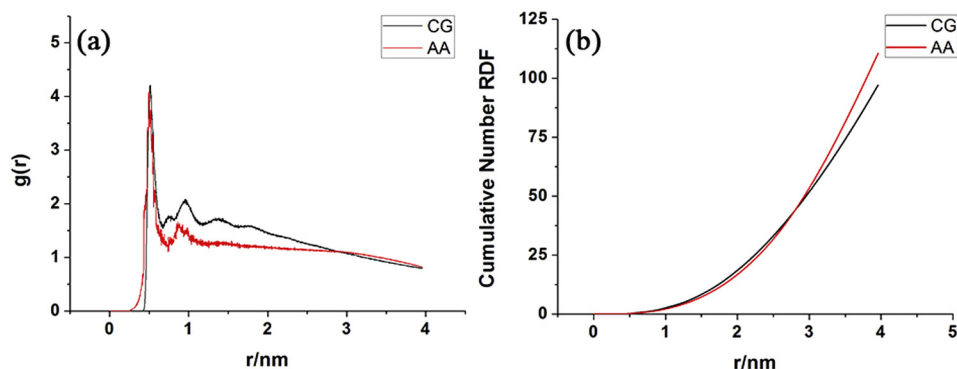

Fig. 2. RDFs (a) and cumulative number RDF (b) of menthol–octanol in the mixed-system of a certain amount of menthol, water and octanol after MD simulations by AA and CG methods.

bilayer systems containing 11 different mass concentrations of menthol were built, 1%, 2%, 3%, 5%, 7%, 10%, 15%, 20%, 30%, 40% and 60%, respectively. Considering the transport of molecules through membrane from the outside of the cell to the inside, menthol molecules were simply randomly placed to replace the same amount of water in the top water layer. Given three-dimensional periodic boundaries, we found that it made no difference to the results. Even for the highest concentration of menthol (60%), only a minute quantity of menthol (less than 1%) would diffuse through the opposite water layer in the following dynamic simulations. Fig. 3(b) shows the side view of a fragment of bilayer packing with 10% menthol.
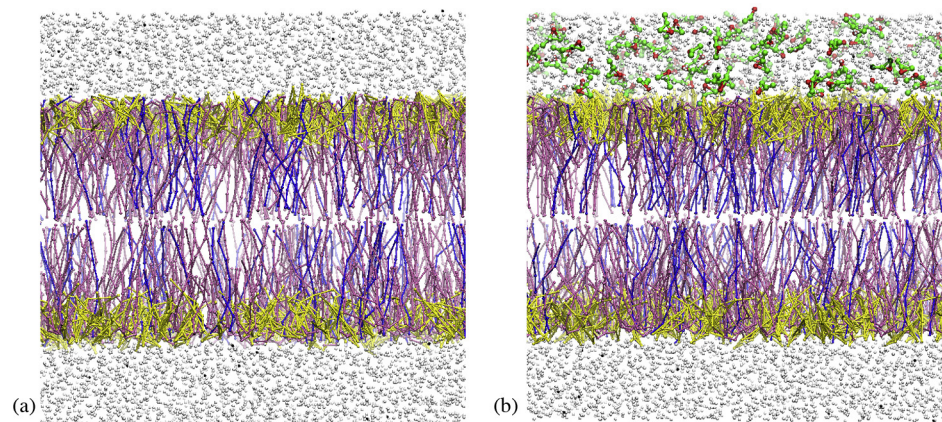

Fig. 3. Snapshots of blank membrane (a) and membrane with 10% menthol (b) before MD simulation. CER, CHOL, FFA and water molecules were represented in pink, yellow, blue and white, respectively. Menthol molecules are colored green, with the polar beads being red. (For interpretation of the references to color in this figure legend, the reader is referred to the web version of this article.)
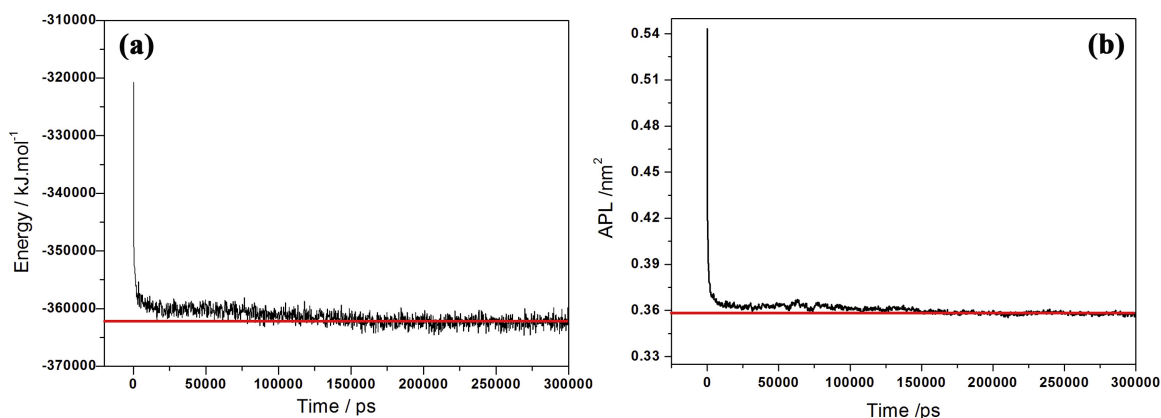
Fig. 4. Total energy (a) and the APL (b) of the blank SC bilayer model during 300 ns simulation at 310 K. The membrane reaches equilibrium within 200 ns, with the constant value of total energy and the APL.

2.5. Simulation details

In this study, we used molecular dynamics simulation at constant temperature and pressure (NPT) ensemble with the GROMACS molecular dynamics package [47]. Before simulation, the structures were relaxed through energy minimization (EM) using the steepest descent algorithm. Potential energy was descended to be negative on the order of 10^5–10^6 and the maximum force no greater than 80 kJ mol^{-1}.

In the production runs, temperature was controlled by v-rescale thermostats coupled separately with the three kinds of lipids, water and menthol molecules with a time constant of 1 ps. When studying the effects of menthol's concentration on the bilayer, the temperature was set to 310 K which was close to the temperature of the human body. Pressure was controlled by berendsen barostat and semiisotropic pressure coupling with time constant of 2 ps and compressibility of 3×10^{-4}/bar. The neighbor searching algorithm was grid and the cut-off distance was 1.4 nm. The method was shift and the cut-off length was chosen to be 1.2 nm for both the van der Waals and electrostatic potentials. The time step was set to 20 fs, and we finally got 300 ns trajectory data from GROMACS simulations.

3. Results

3.1. Equilibration and morphology of the blank SC bilayer model

Before discussing the effect of menthol, we investigated the equilibration of the SC bilayer model. We use total energy and area of per lipid (APL) to evaluate whether the systems have reached equilibrium within simulation times. APL is calculated by dividing the interfacial area of the bilayer (the xy plane) by the number of lipids in each leaflet. Here we plot the total energy and the APL of the blank SC bilayer model through the 300 ns simulation. The results (Fig. 4) shows that the membrane reaches equilibrium within 200 ns, which demonstrates the simulation timescale (300 ns) to be sufficient.

We also took a general look at the membrane morphology. In Fig. 5(a) we can see that after a 300 ns dynamic simulation at 310 K, the sphingosine and fatty acid tails of CER (pink molecules) arranged themselves with an opening angle V-shaped structure, consistent with Dahle'n's work [44]. The single chain FFA (blue molecules) arranged orderly by packing with the tails of CER, thus increasing the density of the hydrocarbon chain packing to a certain degree. CHOL (yellow molecules), on the other hand, due to its shorter length structure, decreased the conformational orderliness of the other lipid chains and thus would provide a degree of fluidity

for the membrane. The whole bilayer formed a gel phase, which was in accordance with the published simulation results [37]. Fig. 5(b) shows the density map of the three kinds of lipids in the bilayer model along z direction. The content of lipids at specified coordinates is represented by the color shades, which turned out to be evenly distributed across the membrane system.

3.2. Concentration effect

3.2.1. Distribution of menthol within the SC bilayer model
3.2.1.1. Density profiles.
To gain insight into the arrangement of menthol within the SC bilayer models, we plotted the density profiles of menthol, the terminal hydrophilic head groups (named AM1, ROH, FAC in Fig. 1.) and the tail-end hydrophobic groups (named C6B, CF in Fig. 1.) of the lipids along the z direction. In order to avoid non-equilibrated results, we analyzed the distribution of the last 100 ns to obtain the average density profiles. Note that the distribution status of menthol were very similar among low concentration groups (only the representative density profiles were shown in Fig. 6). The beads of lipids in upper and sub layer were distinguished by dash line and solid line in the profiles.

We can see that the menthol molecules readily penetrates into the bilayer at each concentration. The distribution results are shown in Fig.S1 in Supplementary Materials. At a lower concentration (0.01–0.20 mass ratio of menthol to water), a large amount of menthol molecules occupies the position between the hydrophobic lipid tails and a relatively small amount are beneath the hydrophilic head groups. The membranes still maintained bilayers with small perturbations forming a 'sandwich' with affinity by menthol molecules. At a higher concentration (30% up), however, menthol molecules tends to mix with the lipids and induces disorder among the lipids. As a result, the lipid structure is dramatically altered, leading to a loss of the bilayer structure.

3.2.1.2. RDFs of different bead-types in menthol with lipids.
Menthol is a amphiphilic molecule with one hydrophilic hydroxyl group (named OM) and three hydrophobic methyl groups (named MCn). It is known that at a lower concentration, menthol molecules mainly occupies two regions of the bilayer (hydrophobic lipid tails and hydrophilic head groups). To further investigate the interaction of menthol with lipids, we calculated the RDFs of OM and MC3 with corresponding part of lipids in the two interaction regions. RDFs are shown at a concentration of 7% in Fig. 7. From Fig. 7(a), we can see that menthol occupies the position beneath the lipid head groups with their hydroxyl groups (OM) oriented towards the lipid head groups. In Fig. 7(b), the RDF peak values of MC3 with hydrophobic tails are higher than that of OM, which demonstrates that the
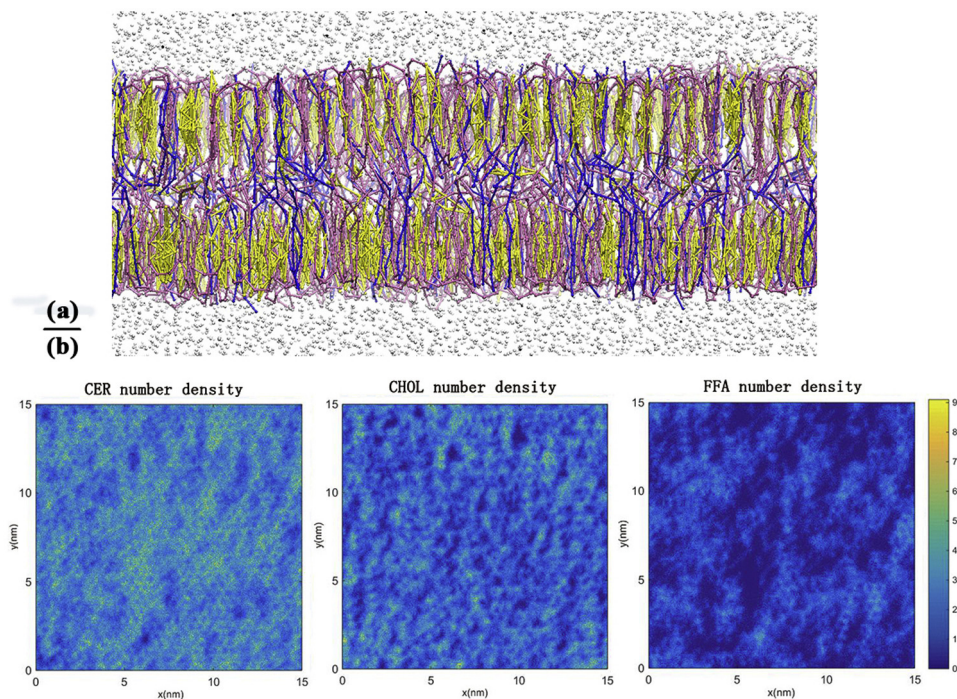
Fig. 5. Morphology of the blank SC bilayer model after 300 ns CG-MD simulation: (a) A snapshot of the blank bilayer model. (b) Density maps of the three kinds of lipids in the bilayer model along *z*-axis. The length and width of the squares represents the *x* and *y*-axis of the simulation boxes, respectively. The content of lipids at the specified coordinates is represented by the color shades, which had been labeled by the color code.
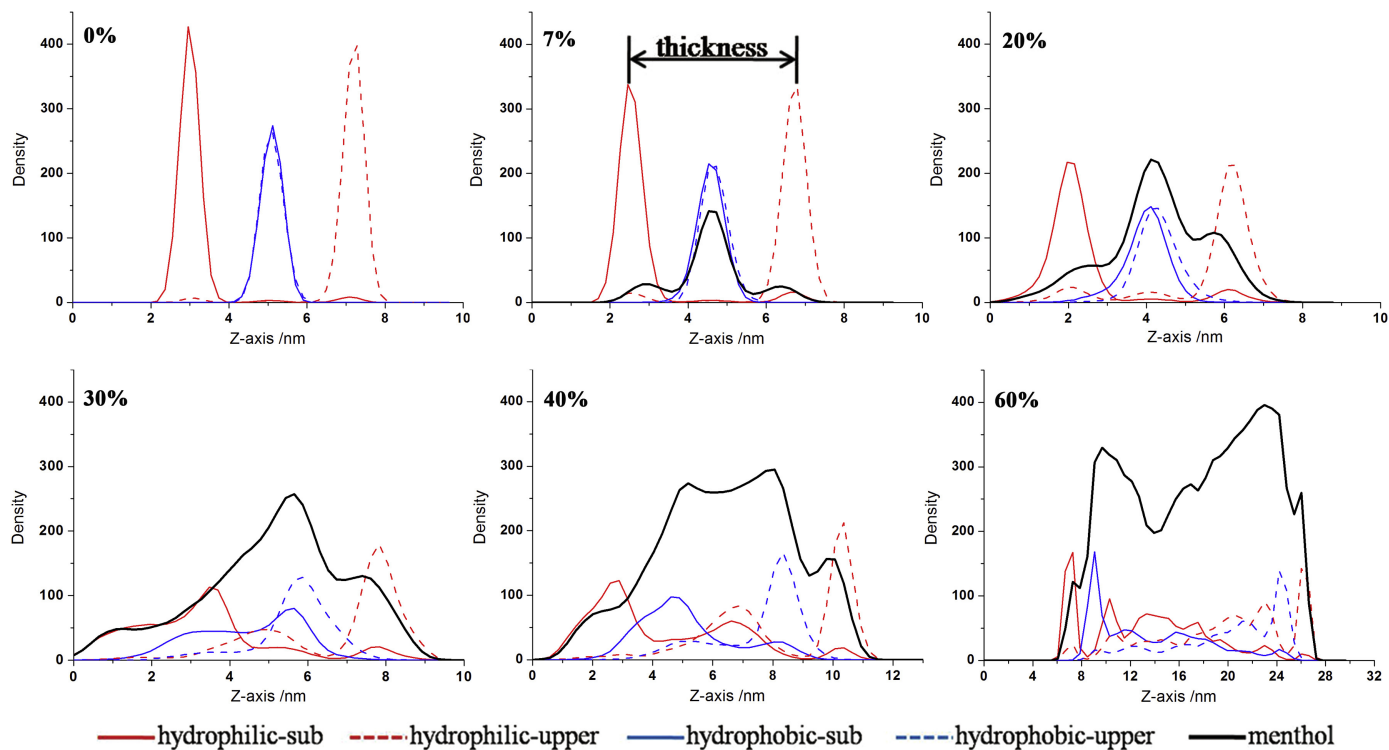

Fig. 6. Average density profiles of bilayer systems with different concentration of menthol during 200–300 ns MD simulation at 310 K. Menthol, the terminal hydrophilic head groups and the tail-end hydrophobic groups are colored black, red and blue, respectively. The beads of lipids in upper and sub layer are distinguished by dash line and solid line. The bilayer thickness can be calculated via the peak–peak distance of hydrophilic head groups in opposite leaflets, discussed in a later part. (For interpretation of the references to color in this figure legend, the reader is referred to the web version of this article.)
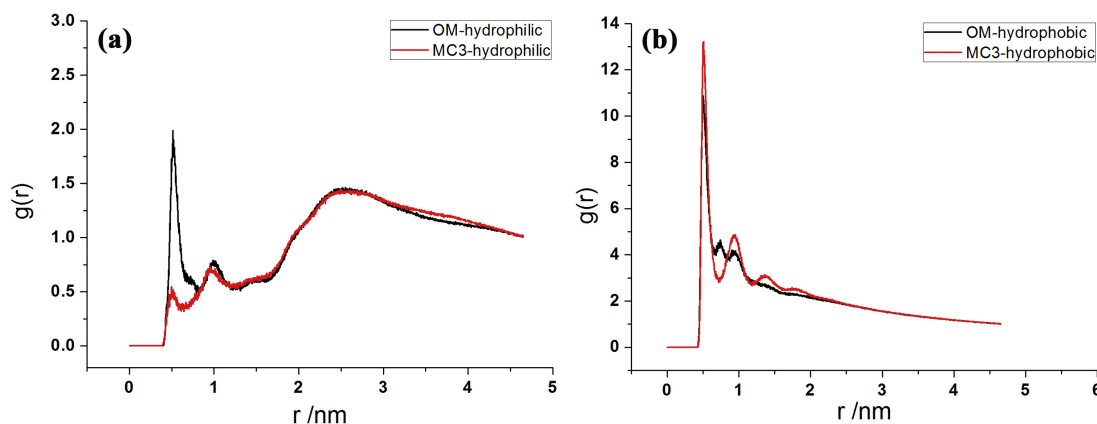
Fig. 7. The RDFs of OM and MC3 with (a) hydrophilic head groups and (b) hydrophobic lipid tails in the bilayer system with 7% menthol after 100 ns MD simulation at 310 K.

methyl groups have more affinity with the lipid tails than with the hydroxyl groups in the central bilayer.

3.2.2. Morphology perturbations of bilayer structure

3.2.2.1. Order parameters. To investigate the perturbation of menthol to the bilayers, we calculated the order parameters of the alkyl chains of lipids (respectively FFA and the two chains of CER, see Fig. 8(a)) under each menthol concentration. The order parameters are calculated using the equation $S_Z = 1/2(3\cos^2\theta_Z - 1)$, where θ_z is the angle between the z axis of the simulation box and the molecular axis under consideration [43]. In Fig. 8. the order of alkyl chains in both CER and FFA decreased with the increase of menthol concentration. This trend is particularly dramatic (with order parameters dropping close to 0 at 60% menthol) as the concentration of menthol increased above 30%. This suggests that penetration of menthol incurred greater disorder in the lipid bilayer, and the lipids will be dramatically disordered when menthol concentration is more than 30%.

3.2.2.2. APL and thickness of bilayer. The APL and bilayer thickness are two fundamental characteristics to describe the property of a bilayer. The APL is a commonly reported quantity describing the compactness of the bilayer. The bilayer thickness is defined as the peak–peak distance of hydrophilic head groups in opposite leaflets of bilayer according to the density profiles (marked in Fig. 6.). The high menthol concentrations (30% up) are not taken into consideration in this part, because the membranes do not maintain bilayers in those conditions based on the findings above.

Fig. 9 shows the APL and thickness of the mixed-lipid bilayer with different concentration of menthol. Using surface pressure-potential-molecular area isotherms, many scientists have calculated the APL of a pure CER2 monolayer to be 0.378–0.420 nm^2 [48–50], which can be used as a reference value for our blank mixed-lipid bilayer obtained from the mesoscopic simulation (0.360 nm^2, the decline in value is possibly caused by the single chain FFA insteading of part of the double chains in CER). We easily found that the APL of the bilayer increased when there are more menthol molecules in the system (Fig. 9(a)), thus causing the bilayer to become loose and flexible. In Fig. 9(b) the results show that at concentrations of 7% or below, menthol causes the bilayer thickness decrease, a result of the perturbation and curvature of the lipid tails. However, the bilayer thickens when the concentration of menthol is above 10%. This is possibly due to a large amount of menthol molecules occupying the position between the two leaflets, which turns out to be the dominant factor to the bilayer thickness under high menthol concentrations.

3.3. Temperature effect

To investigate the effect of temperature on interactions of menthol with the SC bilayer membrane, we chose the system with 7% menthol to run dynamics simulation at six different simulation temperatures (273 K, 285 K, 298 K, 310 K, 323 K and 335 K). This is because the bilayer has relatively well-distributed structure and flexible properties with that concentration of menthol.

3.3.1. Diffusion property of menthol

Mean square displacement (MSD) is the most common measurement of the spatial extent of random motion. This provides an easy way to compute the diffusion constant which is determined by linear regression of the MSD [43]. Here we calculate the MSD and diffusion constant of menthol to describe the permeation ability under different temperatures, shown in Fig. 10. We found that the MSD and diffusion constant of menthol increased with temperature. This suggests that a rise in temperature can promote the penetrating progress of menthol.

3.3.2. Morphological changes of bilayer

To obtain a robust understanding of the mixed-lipid bilayers, the order parameters, the APL and the bilayer thickness were calculated to quantify the structural ordering at different temperatures.

The order parameters of both CER and FFA show a clear drop when temperature increases (Fig. 11). This points to the loss of orientation of lipid tails of a bilayer with a fluid-like tail structure. In Fig. 12 the results show that the APL climbed while the bilayer thickness decreases when temperature goes up. This corresponds to the loosening of lipid head groups and the increased flexibility of the membrane. This also explains why menthol readily penetrates into the bilayer when temperature increases.

4. Discussion and conclusions

In this study, we have presented a series of coarse-grained molecular dynamics simulations to investigate the interaction of menthol with a mixed skin-lipid bilayer model consisting of three components of stratum corneum lipid layers, namely CER2 24:0, FFA 24:0 and CHOL in a 2:2:1 molar ratio. We systematically altered the menthol concentration from 1% to 60% (m/m), and then studied the effect of temperature from 273 K to 335 K in a system with 7% menthol.

Compared with the commonly-used methods (such as differential scanning calorimetry, X-ray diffraction, transmission electron microscope, etc.) which indirectly investigating the penetration enhancing mechanism of PEs, MD simulations can provide us with visual results of the interaction of menthol with SC lipids and gen-
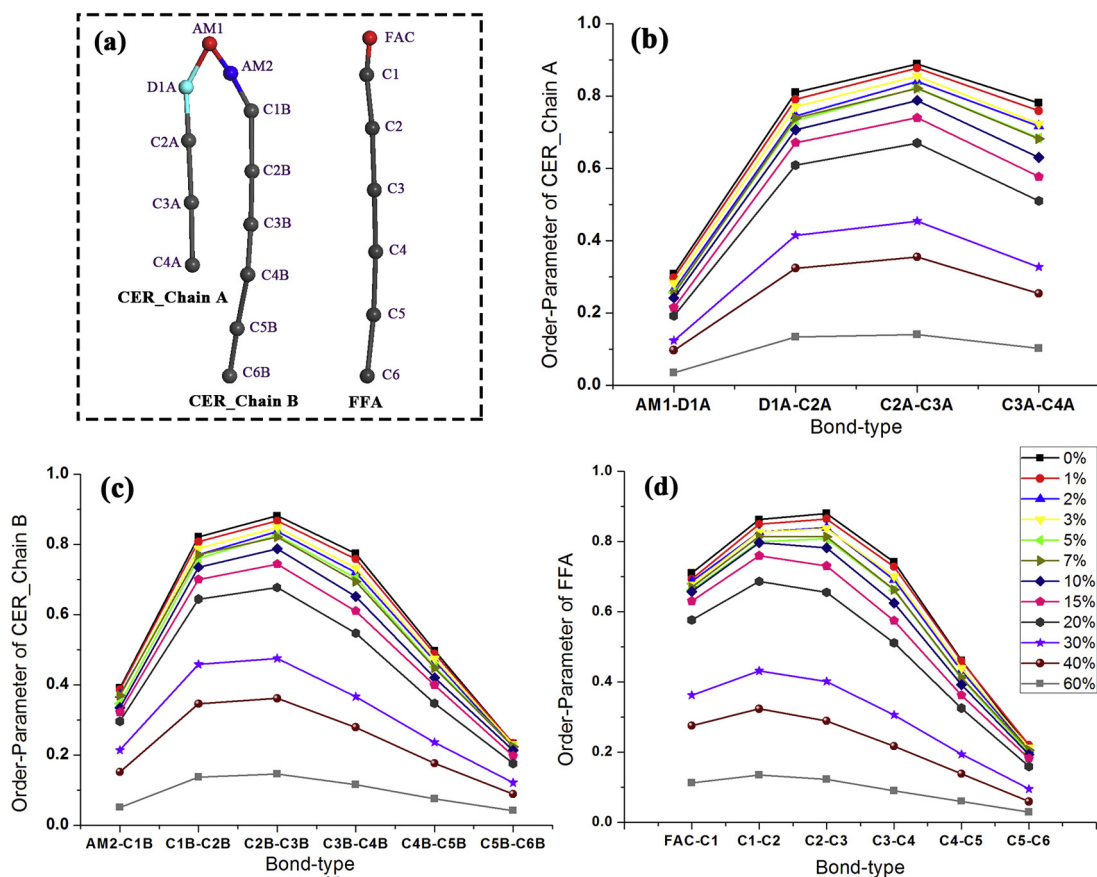
Fig. 8. (a) Label of each bead of CER and FFA. The order parameters of two chains of CER(b, c) and FFA (d) in the systems with different menthol concentrations after 300 ns MD simulation at 310 K.

erate quantitative data of the change of SC. Here, density profiles, RDFs and the MSD were used to investigate the behavior of menthol within the SC bilayers and the membrane structure was evaluated by the order parameters, the APL and the bilayer thickness.

We found that menthol has great affinity to the hydrophobic lipid tails, and some affinity to the hydrophilic head groups as well. This is presumably due to its amphiphilicity. The presence of menthol at any concentration could fluidize the bilayer membrane, leading to the perturbing and disordering of lipid tails to varying degrees. At low concentrations (below 7%), menthol reduced the bilayer thickness by perturbing the lipid tails and increasing the lipid head group area (menthol resided below the lipid head

groups and pushed the head groups apart so the area of per lipid increased). As a consequence, the tail region of the membrane became sparser which enabled the tails of neighboring lipids to expand into an effectively larger volume. At medium concentration (10% to 20%), menthol also caused bilayer lipids loosening and lateral expansion. However, bilayer thickness was increased at the same time (mainly by occupying the position between two leaflets). In both cases, menthol caused the bilayer to become floppier and hence more readily amenable to bending. This leads to improved penetration of agents through the membrane. At high concentrations (30% and more), however, the lipid structure was dramatically altered and the membrane could no longer maintain bilayer struc-
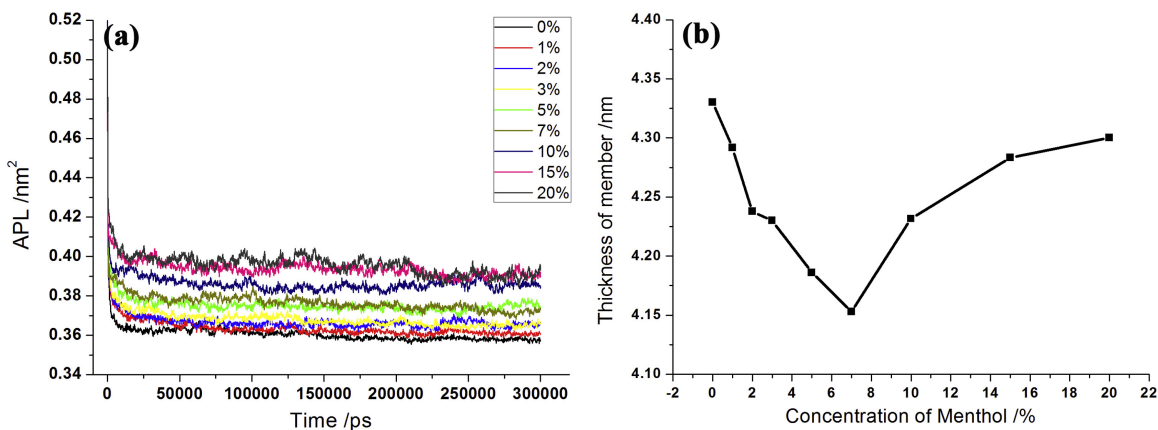

Fig. 9. The (a) APL and (b) thickness of bilayers with different menthol concentration at 310 K.
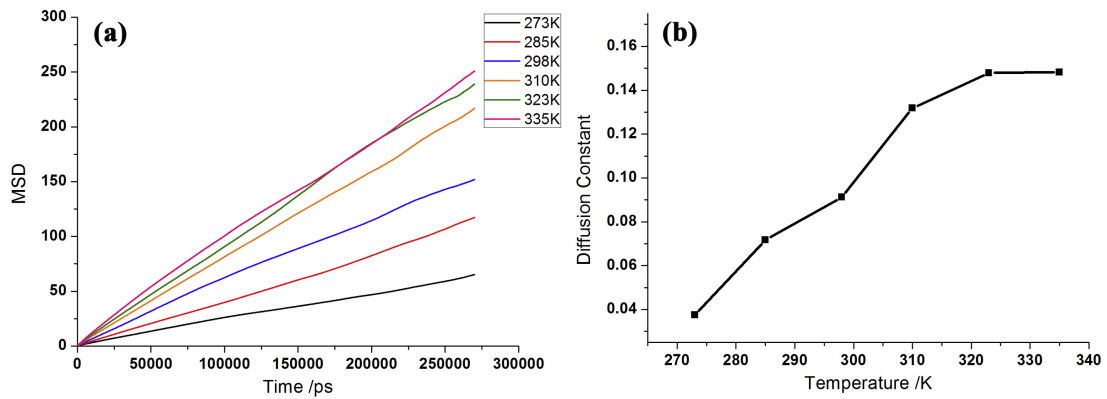
Fig. 10. The (a) MSD and (b) diffusion constant of menthol in the system with 7% menthol at different temperatures.
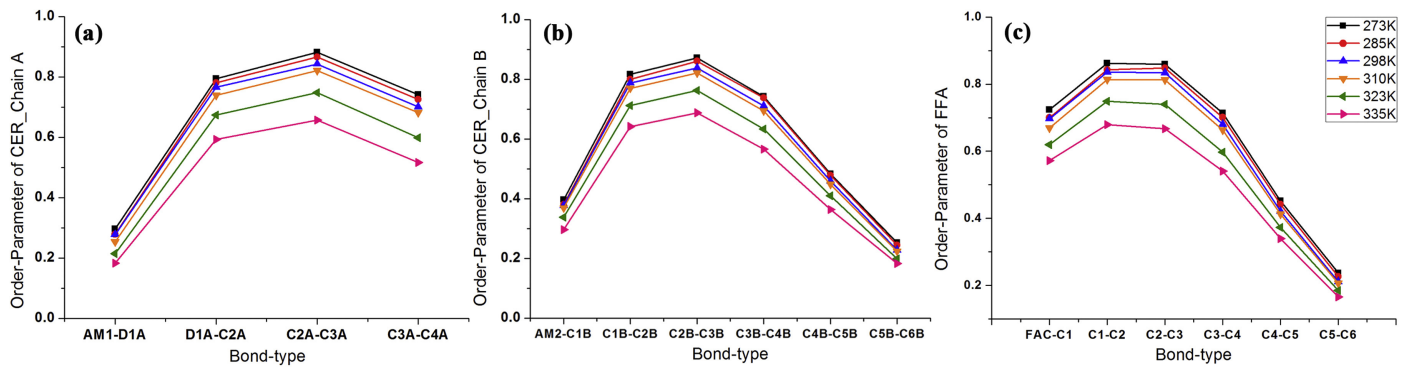

Fig. 11. The order parameters of two chains of CER (a, b) and FFA (c) in the system with 7% menthol after 300 ns MD simulation at different temperatures.

ture. Unlike the effects of other penetration enhancers (i.e. DMSO, ethanol, etc., in high concentrations) to DPPC, POPC or POPE membranes [51–53], menthol completely mixed with the lipids rather than forming water pores or inducing micelle structures.

The morphology perturbation effect on bilayer structures caused by menthol found in this study is in consistent with the works of Wang and Dai [14] and Liang [15]. Wang found that menthol makes the permutation of SC gradually loosened and rumpled by optical microscope. Liang employed multiple methods (scanning electron microscopy, transmission electron microscopy and Fourier Transform Infrared Spectrometer) and found that menthol disturbed the ordered arrangement of SC, widened the space of SC, and rarefied the structure. The normal lamellar-membrane structure of lipids mostly or even completely disappeared and an obviously thickened structure appeared, suggesting that menthol

increased the permeability of the skin. Those findings are completely agreed with our simulation results about the perturbations of menthol to bilayers, and can prove the validity of our simulation method to some extent.

Furthermore, Xu Y [54] used modified Franz diffusion cells to explore the penetration enhancing effect of menthol for lidocaine in gel. Three concentrations of menthol (1%, 3%, 5%, respectively) are taken into consideration, and the results showed that the maximum penetrating enhancement was obtained with 3% menthol, rather than 1% or 5%. This finding indicates that a rise in concentration within a specific range could improve the penetration enhancing ability of menthol, which has the same tendency of out simulation results. To further determine how menthol molecules interact with the fine structure of lipids on a molecular level, all atom MD simulations need to be employed.
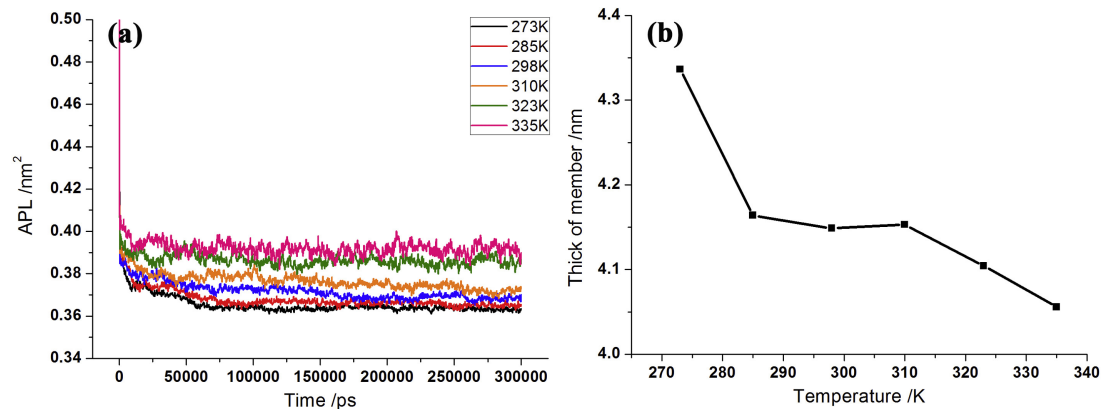

Fig. 12. The (a) APL and (b) thickness of the bilayers with 7% menthol at different temperatures.

When examining the effect of temperature, our results showed that a rise in temperature would promote the penetrating progress of menthol with a significant increase in diffusion constant. The bilayer became floppier when temperature got increased, accompanied with a fall in membrane thickness, an increase in the APL and disordering and enhanced interdigitation of lipid alkane chains. This indicated that menthol affected bilayers more efficiently under higher temperature and thus could more readily promote the penetrating efficiency of drugs.

In short, a rise in temperature and concentration within a specific range could improve the penetration enhancing ability of menthol. Given the pharmacological function of menthol with other drugs and the human tolerance of heat, it is important to identify an optimal concentration and a relatively high temperature in the clinical application of menthol transdermal preparations. We have provided not only some molecular basis for menthol's penetration enhancing effects on mesoscopic level, but also some assistance for development and applications of menthol as a PE. In addition, we have proved the validity of adopting the mixed-lipid bilayer model of SC in future investigations of penetration enhancement mechanism of traditional Chinese medicine with MD simulations, whose property is closer to the real human SC than pure lipid bilayer models.

Acknowledgments

Appendix A. Supplementary data

Supplementary data associated with this article can be found, in the online version, at http://dx.doi.org/10.1016/j.jmgm.2015.06.005

References

[1] P. Karande, S. Mitragotri, Enhancement of transdermal drug delivery via synergistic action of chemicals, Biochim. Biophys. Acta 1788 (2009) 2362–2373.

[2] M.R. Prausnitz, R. Langer, Transdermal drug delivery, Nat. Biotechnol. 26 (2008) 1261–1268.

[3] C. Ren, L. Fang, L. Ling, Q. Wang, S. Liu, L.G. Zhao, Z. He, Design and in vivo evaluation of an indapamide transdermal patch, Int. J. Pharm. 370 (2009) 129–135.

[4] A. Samad, Z. Ullah, M.I. Alam, M. Wais, M.S. Shams, Transdermal drug delivery system: patent reviews, Recent Pat. Drug Delivery Formul. 3 (2009) 143–152.

[5] B.W. Barry, Dermatological Formulations Percutaneous Absorption, Marcel Dekker, New York and Basel, 1983.

[6] B.W. Barry, A.C. Williams, in: J. Swarbrick, J.C. Boylan (Eds.), Permeation Enhancement Through Skin, in Encyclopedia of Pharmaceutical Technology, Vol. 11, Marcel Dekker, New York and Basel, 1995.

[7] M.R. Prausnitz, Microneedles for transdermal drug delivery, Adv. Drug Delivery Rev. 56 (2004) 581–587.

[8] A.T. Rashmi, Y.P. Wang, B.M. Bozena, Essential Oils and Terpenes, in Percutaneous Penetration Enhancers, in: W.S. Eric, I.M. Howard (Eds.), Second Edition-CRC Press, New York, 2005, Chapter 13.

[9] S.O. Mónica, L. Lucía, B.P. Nora, B.D. Nora, Effects of dimethylformamide and L-menthol permeation enhancers on transdermal delivery of quercetin, Pharm. Dev. Technol. 12 (2007) 481–484.

[10] Y.S. Krishnaiah, M.S. Kumar, V. Raju, M. Lakshmi, B. Rama, Penetration-enhancing effect of ethanolic solution of menthol on transdermal permeation of ondansetron hydrochloride across rat epidermis, Drug Delivery 15 (2008) 227–234.

[11] M. Abu Hena Mostofa Kamal, N. Iimura, T. Nabekura, S. Kitagawa, Enhanced skin permeation of salicylate by ion-pair formation in non-aqueous vehicle and further enhancement by ethanol and L-menthoL, Chem. Pharm. Bull. 54 (2006) 481–484.

[12] S.T. Narishetty, R. Panchagnula, Effect of L-menthoL and 1,8-cineole on phase behavior and molecular organization of SC lipids and skin permeation of zidovudine, J. Controlled Release 102 (2005) 59–70.

[13] W. Cai, D. Lin, Effect of the various concentration of azone and menthol on the in vitro percutaneous penetration of terbinafine through excised canine epidermis, Acta Veterinaria et Zootechnica Sinica 40 (2009) 1249–1252, Chinese.

[14] J. Wang, D. Dai, The Effect of menthol on the keratodermia structure, J. Jinling Inst.Technol. 29 (2013) 79–82, Chinese.

[15] Q. Liang, Study on the Penetration-enhancing Effects of Menthol and its Mechanisms, Master's thesis of Guangdong Pharmaceutical University, 2009.

[16] R. Notman, J. Anwar, Breaching the skin barrier-insights from molecular simulation of model membranes, Adv. Drug Delivery Rev. 65 (2013) 237–250.

[17] H.I. Lngolfsson, C.A. Lopez, J.J. Uusitalo, D.H. de Jong, S.M. Gopal, X. Periole, S.J. Marrink, The power of coarse graining in biomolecular simulations, Wiley Interdiscip Rev. Comput. Mol. Sci. 4 (2014) 225–248.

[18] S.J. Marrink, H.J. Risselada, S. Yefimov, D.P. Tieleman, A.H. de Vries, The MARTINI force field: coarse grained model for biomolecular simulations, J. Phys. Chem. B 111 (2007) 7812–7824.

[19] L. Monticelli, S.K. Kandasamy, X. Periole, R.G. Larson, D.P. Tieleman, S.J. Marrink, The Martini coarse-grained force field: extension to proteins, J. Chem.Theory Comput. 4 (2008) 819–834.

[20] L.O.C.A. Pez, A.J. Rzepiela, A.H. de Vries, L. Dijkhuizen, P.H. Hünenberger, S.J. Marrink, Martini coarse-grained force field: extension to carbohydrates, J. Chem. Theory Comput. 12 (2009) 3195–3210.

[21] D.H. de Jong, G. Singh, W.F.D. Bennett, C. Arnarez, T.A. Wassenaar, L.V. Schäfer, X. Periole, D.P. Tieleman, S.J. Marrink, Improved parameters for the martini coarse grained protein force field, J. Chem.Theory Comput. 1 (2012) 687–697.

[22] S.J. Marrink, D.P. Tieleman, Perspective on the martini model, Chem. Soc. Rev. 42 (2013) 6801–6822.

[23] G. Srinivas, R.V. Mohan, A.D. Kelkar, Polymer micelle assisted transport and delivery of model hydrophilic components inside a biological lipid vesicle: a coarse-grain simulation study, J. Phys. Chem. B 10 (2013) 12095–12104.

[24] E.R. May, D.I. Kopelevich, A. Narang, Coarse-grained molecular dynamics simulations of phase transitions in mixed lipid systems containing LPA, DOPA, and DOPE lipids, Biophys. J. 94 (2008) 878–890.

[25] S. Nawaz, C. Paola, Coars-graining poly(ethylene oxide)-poly(propylene oxide)-poly(ethylene oxide) (PEO-PPO-PEO) block copolymers using the martini force field, J. Phys. Chem. B 118 (2014) 1648–1659.

[26] E.M. Curtis, C.K. Hall, Molecular dynamics simulations of DPPC bilayers using 'LIME', a new coarse-grained model, J. Phys. Chem. B 117 (2013) 5019–5030.

[27] R.S. Davis, P.B. Sunil Kumar, M.M. Sperotto, M. Laradji, Predictions of phase separation in three-component lipid membranes by the martini force field, J. Phys. Chem. B 117 (2013) 4072–4080.

[28] http://md.chem.rug.nl/cgmartini

[29] P.M. Elias, Epidermal lipids barrier function, and desquamation, J. Invest. Dermatol. 80 (1983) 44–49.

[30] A.S. Michaels, S.K. Chandrasekaran, J.E. Shaw, Drug permeation through human skin: theory and in vitro experimental measurement, AIChE J. 21 (1975) 985–996.

[31] K.C. Madison, D.C. Swartzendruber, P.W. Wertz, D.T. Downing, Presence of intact intercellular lipid lamellae in the upper layers of the stratum corneum, J. Invest. Dermatol. 88 (1987) 714–718.

[32] J.A. Bouwstra, M. Ponec, The skin barrier in healthy and diseased state, Biochimca et Biophysica Acta 1758 (2006) 2080–2095.

[33] A.P. Lyubartsev, A.L. Rabinovich, Recent development in computer simulations of lipid bilayers, Soft Matter 7 (2011) 25–39.

[34] A.A. Gurtovenko, J. Anwar, I. Vattulainen, Defect-mediated trafficking across cell membranes: insights from in silico modeling, Chem. Rev. 110 (2010) 6077–6103.

[35] R. Notman, W.K. den Otter, M.G. Noro, W.J. Briels, J. Anwar, The permeability enhancing mechanism of DMSO in ceramide bilayers simulated by molecular dynamics, Biophys. J. 93 (2007) 2056–2068.

[36] J. Shah, J.M. Atienza, A.V. Rawlings, G.G. Shipley, Physial properties of ceramides: effect of fatty acid hydroxylation, J. Lipid Res. 36 (1995) 1945–1955.

[37] M. Höltje, T. Forster, B. Brandt, T. Engels, W. von Rybinski, H.D. Höltje, Molecular dynamics simulations of stratum corneum lipid models: fatty acids and cholesterol, Biochimca et Biophysica Acta 1511 (2001) 156–167.

[38] C. Das, M.G. Noro, P.D. Olmsted, Simulation studies of stratum corneum lipid mixtures, Biophys. J. 97 (2009) 1941–1951.

[39] C. Das, P.D. Olmsted, M.G. Noro, Water permeation through stratum corneum lipid bilayers from atomistic simulations, Soft Matter 5 (2009) 4549–4555.

[40] T. Engelbrecht, T. Hau, K. Su, A. Vogel, M. Roark, S.E. Feller, R.H.H. Neubert, B. Dobner, Characterisation of a new ceramide EOS species: synthesis and investigation of the thermotropic phase behaviour and influence on the bilayer architecture of stratum corneum lipid model membranes, Soft Matter 7 (2011) 8998–9011.

[41] http://md.chem.rug.nl/cgmartini/index.php/paramet-rzining-new-molecule

[42] Accelrys I. Materials Studio Accelrys Software Inc., San Diego, 2010.

[43] Gromacs User Manual (Version 4.6.3., Edited by Hess, B., van der Spoel, D., and Lindahl, E.).

[44] B. Dahleín, I. Pascher, Molecular arrangements in sphingolipids, Thermotropic phase behav. Tetracosanoylphytosphingosine. Chem. Phys. Lipids 24 (1979) 119–133.

[45] L. Martínez, R. Andrade, E.G. Birgin, J.M. Martínez, Packmol a package for building initial configurations for molecular dynamics simulations, J. Comput. Chem. 30 (2009) 2157–2164.

[46] W. Humphrey, A. Dalke, K. Schulten, VMD Visual molecular dynamics, J. Mol. Graphics 14 (1996) 33.

[47] D. van der Spoel, E. Lindahl, B. Hess, G. Groenhof, A.E. Mark, H.J.C. Berendsen, GROMACS: fast, flexible and free, J. Comput. Chem. 26 (2005) 1701–1718.

[48] L. Scheffer, I. Solomonov, M. Jan Weygand, K. Kjaer, L. Leiserowitz, L. Addadi, Structure of cholesterol/ceramide monolayer mixtures: implications to the molecular organization of lipid rafts, Biophys. J. 88 (2005) 3381–3391.

[49] H.L. Brockman, M.M. Momsen, R.E. Brown, L.L. He, J. Chun, H.S. Byun, R. Bittman, The 4,5-double bond of ceramide regulates its dipole potential, elastic properties, and packing behavior, Biophys. J. 87 (2004) 1722–1731.

[50] H. Löfgren, I. Pascher, Molecular arrangements of sphingolipids, Monolayer Behav. Ceramides Chem. Phys. Lipids 20 (1997) 273–284.

[51] R. Notman, M. Noro, B. O'Malley, J. Anwar, Molecular basis for dimethylsulfoxide (DMSO) action on lipid membranes, J. Am. Chem. Soc. 128 (2006) 13982–13983.

[52] A.A. Gurtovenko, J. Anwar, Interaction of ethanol with biological membranes: the formation of non-bilayer structures within the membrane interior and their significance, J. Phys. Chem. B 113 (2009) 1983–1992.

[53] Q. Yin, X. Shi, H. Ding, X. Dai, G. Wan, Y. Qiao, Interactions of borneol with DPPC phospholipid membranes: a molecular dynamics simulation study, Int. J. Mol. Sci. 15 (2014) 20365–20381.

[54] Y.Y. Xu, W.Q. Liang, Effects of menthol and azone on percutaneous permeation of lidocaine in gel, China Pharm. 14 (2003) 337–338, Chinese.